OFFICE OF NAVAL RESEARCH

Contract N00014-91-J-1641

R&T Code 313W001

TECHNICAL REPORT NO. 69

Nanosecond Laser Induced Tunneling and Atom Deposition-An STM Application to Nanofabrication

by

V. A. Ukraintsev and J.T. Yates, Jr.

Submitted To

J. Appl. Phys.

Surface Science Center
Department of Chemistry
University of Pittsburgh
Pittsburgh, PA 15260

February 27, 1996

DISCLAIMER NOTICE

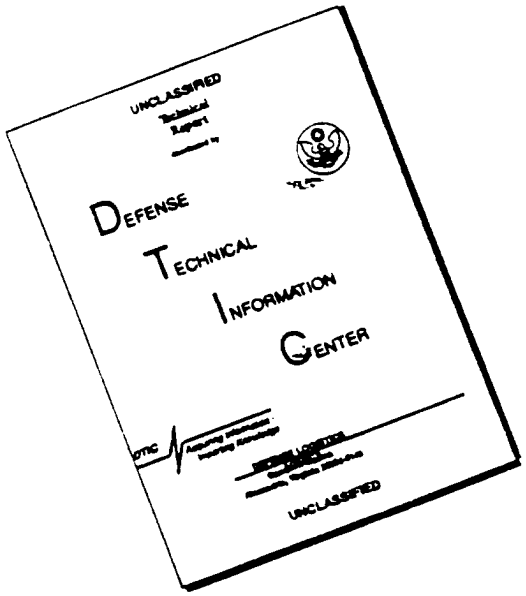

THIS DOCUMENT IS BEST QUALITY AVAILABLE. THE COPY FURNISHED TO DTIC CONTAINED A SIGNIFICANT NUMBER OF PAGES WHICH DO NOT REPRODUCE LEGIBLY.

REPORT DOCUMENTATION PAGE

Form Approved
OMB No. 0704-0188

1. AGENCY USE ONLY (Leave blank)	2. REPORT DATE	3. REPORT TYPE AND DATES COVERED
	February 27, 1996	Preprint

4. TITLE AND SUBTITLE
Nanosecond Laser Induced Tunneling and Atom Deposition-An STM Application to Nanofabrication.

5. FUNDING NUMBERS
N00014-91-J-1641

6. AUTHOR(S)
V.A. Ukraintsev and J.T. Yates, Jr.

7. PERFORMING ORGANIZATION NAME(S) AND ADDRESS(ES)
Surface Science Center
Department of Chemistry
University of Pittsburgh
Pittsburgh PA 15260

8. PERFORMING ORGANIZATION REPORT NUMBER

9. SPONSORING/MONITORING AGENCY NAME(S) AND ADDRESS(ES)
Office of Naval Research
Chemistry Division, Code 313
800 North quincy Street
Arlington, Virginia 22217-5000

10. SPONSORING/MONITORING AGENCY REPORT NUMBER

11. SUPPLEMENTARY NOTES

12a. DISTRIBUTION/AVAILABILITY STATEMENT

12b. DISTRIBUTION CODE

13. ABSTRACT *(Maximum 200 words)*

Nanosecond laser pulses, with 2.33 eV photon energy and ~ 0.6 MW/cm^2 radiation flux, have been used to initiate a transient increase of tunneling current between the tip and sample surface in an ultrahigh vacuum STM apparatus. As the laser power is increased to ~ 2.5 MW/cm^2, single atom transfer from the tip to a silicon surface occurs. For both polarities the laser induced tunneling current is linear with laser pulse energy up to ~ 0.6 MW/cm^2. A transient tunneling current up to 15 μA has been observed. The similarity of the laser induced transient tunneling for both polarities, and hence its independence on material, suggest that the same mechanism is operative in both directions of tunneling. Both ballistic electron tunneling and band bending effects have been considered in the analysis of the electron transfer. It is proposed, however, that pulse laser heating of the tip causes this transient increase of the tunneling current due to a transient thermal expansion, reducing the tip-sample tunneling distance. The increase in tunneling current may lead to additional Nottingham heating of the tip apex.

At a laser flux of 2.5 MW/cm^2, single atom transfer between the W tip and the silicon surface occurs. The number of atoms transferred can be controlled by the laser flux, and the transfer process is virtually independent of the tip-sample bias polarity. Since a maximum tip temperature of 650 K is estimated during the pulse, W atom transfer must occur under the influence of strong W-Si chemical interaction. The speed of the pulse laser atom transfer (8 nsec) exceeds by orders of magnitude the transfer speed which could be achieved by pulsing the STM piezo drive.

14. SUBJECT TERMS			15. NUMBER OF PAGES
			16. PRICE CODE
17. SECURITY CLASSIFICATION OF REPORT	18. SECURITY CLASSIFICATION OF THIS PAGE	19. SECURITY CLASSIFICATION OF ABSTRACT	20. LIMITATION OF ABSTRACT

Submitted to: J. Appl. Phys.
February 27, 1996

Nanosecond Laser Induced Tunneling and Atom Deposition - An STM Application to Nanofabrication.

V. A. Ukraintsev and J. T. Yates, Jr.

University of Pittsburgh
Department of Chemistry
Surface Science Center
Pittsburgh, PA 15260

Nanosecond Laser Induced Tunneling and Atom Deposition - An STM Application to Nanofabrication.

V. A. Ukraintsev and J. T. Yates, Jr.

University of Pittsburgh
Department of Chemistry
Surface Science Center
Pittsburgh, PA 15260

Nanosecond laser pulses, with 2.33 eV photon energy and ~ 0.6 MW/cm^2 radiation flux, have been used to initiate a transient increase of tunneling current between the tip and sample surface in an ultrahigh vacuum STM apparatus. As the laser power is increased to ~ 2.5 MW/cm^2, single atom transfer from the tip to a silicon surface occurs. For both polarities the laser induced tunneling current is linear with laser pulse energy up to ~ 0.6 MW/cm^2. A transient tunneling current up to 15 μA has been observed. The similarity of the laser induced transient tunneling for both polarities, and hence its independence on material, suggest that the same mechanism is operative in both directions of tunneling. Both ballistic electron tunneling and band bending effects have been considered in the analysis of the electron transfer. It is proposed, however, that pulse laser heating of the tip causes this transient increase of the tunneling current due to a transient thermal expansion, reducing the tip-sample tunneling distance. The increase in tunneling current may lead to additional Nottingham heating of the tip apex.

At a laser flux of 2.5 MW/cm^2, single atom transfer between the W tip and the silicon surface occurs. The number of atoms transferred can be controlled by the laser flux, and the transfer process is virtually independent of the tip-sample bias polarity. Since a maximum tip temperature of 650 K is estimated during the pulse, W atom transfer must occur under the influence of

strong W-Si chemical interaction. The speed of the pulse laser atom transfer (8 nsec) exceeds by orders of magnitude the transfer speed which could be achieved by pulsing the STM piezo drive.

1. *Introduction*

A variety of techniques have been invented since the first fabrication of a nanometer-scale structure controlled by a scanning tunneling microscope (STM), performed by Ringger and co-workers in 1985.[1] A comprehensive review of modern methods used in nanofabrication was written recently by R. Wiesendanger.[2] The majority of the techniques can be classified according to the mechanism of the "writing" phenomenon. The classes are: (a) mechanical or atomic force surface modifications; (b) electron-stimulated surface modifications; (c) electric field induced surface modifications; and (d) thermally induced surface modifications. However, in many cases the exact mechanism of the nanomodification is unknown or seems to be a combination of mechanisms.

Laser interaction with point-contact metal-vacuum-metal or metal-insulator-metal diodes was studied extensively during many years before the STM invention (see for example ref. 3). A laser in combination with the STM was used successfully to gain a fundamental understanding of the tip-surface interaction[4] as well as to provide new insight into the process of the photo excited carrier recombination.[5] As a result several methods of photo-assisted scanning tunneling microscopy and spectroscopy have been developed.[2]

Despite of the prominent interest to the photo-assisted STM very little is known about processes at the STM tip-sample junction stimulated by a pulse

laser[6,7] and only several attempts have been made to use photon radiation for nanofabrication[6,7,8,9,10,11].

Betzig *et al.*[9] and Mamin *et al.*[10,11] have used a laser to heat a tip of an atomic force microscope or the apex of a tapered optical fiber of the near field scanning optical microscope. The heated tip or fiber can be used then for magneto-optic writing[9] or for thermo-mechanical nanoindentation on polymeric surfaces.[10,11] A spatial resolution of ~ 100 nm has been achieved.

Yau *et al.*[6] employed a tunable nanosecond pulsed laser with intensity of ~ 10^8 W/cm^2 focused "just in front of the tunneling gap" to photodissociate trimethylaluminum (TMA) molecules and to ionize subsequently the aluminum atoms. An electric field existing in the tunneling gap "steers" the ionized species to the substrate surface. Protrusions and depressions with sizes down to ~ 30 Å have been obtained on a graphite surface as a result of the photo-assisted nanofabrication. The high, 10^8 W/cm^2, laser intensity is necessary in these experiments because of the multiphoton nature of the aluminum atom ionization.[12] Under such conditions the processes at the tip-sample junction are barely controllable and unpredictable (see Section 4).

Photo-assisted etching of a CdSe film underneath an STM tip has been reported by Lin and Bard.[8] A mechanism for the field assisted photo-dissociation of the CdSe is proposed.

Intriguing data have been published by Kazmerski,[9] who reported the photo-assisted selective single atom removal from a (220) $CuInSe_2$ surface. The experimental procedure, conditions, and the data evaluation methods are not given in detail, and no mechanism for the atom transport is presented.

In this paper we report on a nanosecond laser induced one-per-pulse atom transfer from STM tip to a Si(001)-(2×1) surface. The highly reproducible deposition of the tip material was obtained in ultrahigh vacuum (UHV) conditions. To understand the mechanism of the atom transfer phenomenon, a transient tunneling current, induced by the nanosecond laser pulse, was measured as a function of the photon flux and the tip-sample bias. A model of the tip-to-surface atom transfer assisted by laser induced tip heating and thermal expansion is proposed.

2. *Experimental*

A UHV chamber with background pressure of 2×10^{-11} Torr was employed for the experiments. The chamber was equipped with the STM (Omicron), a cylindrical mirror analyzer Auger spectrometer (Model 15-110, Physical Electronics Industries Inc.), a quadrupole mass-spectrometer (100C, UTI) and an ion sputtering gun. The Si(001) crystal (p-type, B-doped, 100 Ω·cm, Virginia Semiconductor) with dimensions $15\times4\times0.3$ mm^3 was cut from a silicon wafer by a diamond scribe, mounted on an etched-in-HCl Ta frame[13], ultrasonicated in pure ethanol, rinsed in deionized water and introduced into the UHV chamber

through the load-lock system. After overnight outgassing at ~ 900 K the native oxide layer was removed from the Si(001) by a short (~ 60 sec) annealing at ~ 1450 K followed by slow (~ 2 K/sec) cooling[13].

STM imaging revealed a well organized (2×1) structure with traces of Ni contamination (see Ref. 13 for details). These Ni induced surface defects were utilized as markers in our nanofabrication experiments.

The second harmonic (λ = 532 nm, hν = 2.33 eV) of the pulsed YAG: Nd^{+3} laser (Continuum) was focused on the apex of the STM tip by employing a quartz lens (f = 50 cm). The laser spot diameter, D_b, was estimated using the second harmonic divergence ($\alpha \cong 5\times10^{-4}$ rad) as $D_b \cong \alpha f \cong 250$ μm. According to the laser technical specification, the laser energy spatial distribution in the focal plane is close to Gaussian.

The laser beam focusing on the tip apex was controlled by a co-aligned telescope with a precision better than ± 50 μm. The pulse energy was measured directly in front of the UHV chamber window by a high sensitivity lithium tantalate detector (818J-09B, Newport). A second detector (818J-50B, Newport) was used to monitor the laser pulse energy stability during the experiments. The second harmonic stability was better than 4%.

The laser beam hits the surface at an incident angle of $\theta_i \sim 80°$. The P-polarization of the laser (with respect to the silicon surface) was used in

experiments reported here. The laser pulse duration is ~ 8 nsec and the repetition rate is 10 Hz.

The laser pulse energy control was accomplished by the adjustment of the Q-switching delay. This method allows one to keep constant the laser spatial distribution as well as the laser spot position at the tip apex. The use of optical filters is not acceptable here because of the high requirements on stability of the laser beam alignment during the experiment, which can not be satisfied by the commercially available filters with transmitted beam deviation of ~ 10^{-4} rad.

The transient tunneling current induced by the laser pulse (8 nsec) can not be measured directly without major changes in the low noise and, hence, low frequency STM electronics. On the other hand, as was proved by modeling, an amount of electricity transferred between the tip and the sample during the short transient tunneling (~ 10^{-8} sec) is equal to an amount of electricity transferred through the feedback of the input amplifier during ~ 10^{-5} sec. This is correct for tunneling currents up to 3 μA with a 50% accuracy.[14] It may be surprising that the circuit designed for measurements in the nA range has a linear response for 3 μA current. The reason for this is the small amount of an electricity transferred during the short pulse, (3 μA × 10^{-8} sec) ≅ 3×10^{-14} C. Assuming the amplifier input capacitance of ~ 5 pF, one estimates the input transient signal as (3×10^{-14} C/ 5×10^{-12} F) ≅ 6×10^{-3} V, which is in the linear range of the amplifier.

If the transferred charge is known, one may estimate the transient tunneling current induced by the laser, assuming the current pulse duration equals ~ 8 nsec (see Section 4).

3. *Results*

Two major phenomena were observed during laser irradiation of the tip-sample junction: (1) a laser induced transient increase of the tunneling current; (2) a laser induced deposition of the tip apex material on the surface. The later was observed with a laser flux on the tip higher than 2.5 MW/cm^2. For the conditions of this experiment, a laser pulse power density of 1 MW/cm^2 = 4 $\mu J/pulse$ = 2.7×10^{24} $photon/cm^2$ sec.

3.1 Charge Transfer at STM Junction

In order to eliminate the remotepossibility of laser induced thermal or photo electron emission, the tip was placed at distance of ~ 1 mm from the positively biased sample and irradiated by the laser with a flux of ~ 10 MW/cm^2. This flux is two times higher than the maximum flux used in the experiments reported below. With the highest possible sample bias of +10 V, no charge transfer was detected above the noise level estimated as 10^{-15} C.

The situation is different if tunneling is established between the tip and the sample. Here, depending on the laser power either only charge transfer occurs, or transfer of both charge and tip material occurs.

Figure 1(a) and 1(b) present the dependence on photon flux (or laser pulse energy) of the transient tunneling current (or the transferred charge), induced by the pulse irradiation of the tip-sample junction. For both negative and positive sample bias voltages the dependencies are similar and virtually linear.

The STM feedback control was on during the entire experiment and the reference current was fixed at 1.0 nA. Since the feedback response time is much longer than the laser pulse duration, the transient tunneling current is virtually undisturbed by the feedback response. Every point in Figures 1(a) and 1(b) was averaged over at least 1000 laser pulses. Despite the tip changes, the various tip positions with respect to the surface, and small alterations in laser beam alignment, the linear dependence was consistently observed in a number of experiments.

If the transferred charge exceeds the 3×10^{-13} C per pulse, the output signal undergoes slow exponential decay which we speculatively attribute to the entire amplifier circuitry charging. The extensive charging leads, finally, to the temporary disability of the STM feedback. This condition occurs after several hundred laser pulses.

Figure 2 shows the transient tunneling current dependence on the sample bias voltage obtained at the constant laser pulse energy of ~ 2.4 μJ. The STM feedback control was on during this experiment and the reference current was fixed at 1.0 nA. Several features, independent of the tip condition and the

surface site beneath the tip, are seen in Figure 2: (1) at high biases ($V > +3$ V; $V < -3$V) the transient tunneling current experiences a steep decay; (2) the absolute value of the transient tunneling current exhibits two anti-symmetric maxima at $V = \pm 3$ V (ref. 15); (3) at bias close to zero a positive transient tunneling current is observed (on average more electrons move from the tip toward the sample than in the opposite direction).

3.1 Atom Transfer at STM Junction

The process of laser induced tip material deposition with atomic level spatial control is demonstrated in Figure 3. The top picture shows the STM image of the Si(001)-(2×1) surface before the laser induced modification. The surface defects serve here as markers.

Figure 3(b) presents the STM image of the same surface region obtained simultaneously with a series of six laser pulses. The laser repetition rate is 10 Hz; the tip moves 42 Å between pulses. The STM feedback response to the high transient tunneling current is apparent in this picture. The tip scans the region from the left to the right and from the bottom to the top. Hence, the deposited atoms are visible already on several horizontal traces recorded immediately after the laser pulse series, Fig. 3(b). The markers relative positions were not changed after the series of the laser pulses and, hence, the imaging is stable during the laser induced surface modification.

The modified Si(001)-(2×1) surface is shown in Figure 3(c). The six single atom depositions aligned along the horizontal line of the scan result from the six laser pulses. The atoms' location with respect to the markers and relative to each other leaves no doubts concerning their origin from the region of the STM tip.

The surface modification was obtained under the following conditions: the sample bias V = -1.3 V; feedback reference current I_0 = 1.0 nA; laser pulse energy $E_p = (12 \pm 2)$ μJ.

The transfer process exhibits a threshold laser energy, $E_{min} \cong (10 \pm 2)$ μJ. The sample bias polarity is not important and virtually the same laser threshold energy was observed for positive sample bias V = +1.3 V.

Starting at a laser energy of $E_p = (15 \pm 3)$ μJ a deposition of several atoms per pulse may be observed. The atoms are deposited then close to each other in the vicinity of the tip apex position during the laser pulse. If the laser energy is high enough, clusters with a height of more than one atomic size are fabricated on the surface. Under no circumstances was laser induced surface atom extraction from the silicon surface or atomic diffusion on the surface observed.

Minor changes in the surface appearance and, hence, in the tip condition were visible during the laser induced surface modification. However, the STM feedback effectively compensates for these changes and, as was mentioned before, the imaging is stable and the tip drift is acceptable.

As soon as the laser energy thresholds for single atom and for multiatom deposition are determined and the laser energy is held in these limits, the process of single atom deposition is very reproducible. Using data available to date the probability of misfunction can be estimated as 5-10 %. The surface defects slightly influence the position of the deposition (Fig. 3) and increase the chance of the multiatom deposition (not shown).

Visualized by the STM, the apparent height and the apparent diameter of the deposited single atom are estimated as (2.25 ± 0.5) Å and (11 ± 2) Å, respectively (Fig. 4). These numbers are clearly different from the height and the diameter of the single silicon adatoms frequently observed on Si(001)-(2x1) disordered by a slight surface contamination and/or by fast cooling (ref. 13). The silicon adatoms on top of Si(001)-(2x1), as seen by STM at similar bias voltage and reference current, have an apparent height of (1.3 ± 0.2) Å and an apparent diameter of (6.7 ± 1) Å.

4. Discussion

In this section we discuss several possible mechanisms of the transient tunneling and the single atom deposition observed during the pulse irradiation of the STM tip-sample junction. Disregarding the intermediate processes, the absorption of the laser energy should finally lead to an increase of the tip and the sample lattice temperatures. Therefore, laser induced heating of both the tip and the sample should be considered.

4.1 Pulse Laser Heating and Thermal Expansion

A scheme of the tip-sample junction irradiated by a laser is presented in Figure 5. Since the incident angle is $\theta_i \sim 80°$ in our geometry, one would expect a larger photon flux and, hence, higher transient temperature on the tip surface rather than on the sample surface. We first discuss the laser heating of the tip.

4.1.1 Tip Heating by Pulse Laser

Three characteristic dimensions should be considered (ref. 16): (i) the photon absorption length, $\lambda_{abs} \sim$ (100-500) Å; (ii) the thermal diffusion length, $\lambda_{th} \sim (\chi\tau_p)^{1/2} \cong 7500$ Å; and (iii) the laser beam size, $D_b \cong 250$ μm. Here $\chi = 0.7$ cm^{2}s^{-1} (ref. 21), the tungsten coefficient of thermal diffusion, and $\tau_p = 8$ nsec the laser pulse duration.

Since $D_b >> \lambda_{th} >> \lambda_{abs}$, steady state heating can not be established during the pulse and, hence , the maximum transient temperature occurs at the end of the laser pulse and is approximately proportional to the laser fluence.[16]

The tip radius, $r_t \sim$ (100-1000) Å, is smaller than λ_{th} and, therefore, the case is not strictly one-dimensional. A three-dimensional (3D) case with an azimuthal symmetry was considered by Miscovsky *et al.*[17] It was found that "the temperature rise in the conical tip due to surface generation of heat varies almost

linearly with laser intensity and heating time and depends strongly on the cone angle and thermal properties."

For a crude estimation of the transient temperature in the λ_{th} vicinity of the tip apex, one may use the following simple expression:

$$\Delta T_{tip} c_p \rho V_{th} \cong A_{th} \times \frac{4E_p(1 - \overline{R})}{\pi D_b^2}, \qquad (1)$$

where c_p and ρ are the heat capacity and the density of the tungsten, respectively; $V_{th} \cong \frac{2\pi(1 - \cos\theta_0)\lambda_{th}^3}{3}$ and $A_{th} \cong \theta_0 \lambda_{th}^2$ are the volume and the cross-section area of the λ_{th} - vicinity of the tip apex, respectively;[18] θ_0 is the tip cone angle in radians; E_p is the laser pulse energy and $\overline{R}$ is the effective reflectivity of the light averaged over the irradiated tip surface and, hence, over different incidence angles.[19]

Using eqn. (1) one gets for the tip apex temperature rise:

$$\Delta T_{tip} \cong \frac{6\theta_0 E_p(1 - \overline{R})}{\pi^2(1 - \cos\theta_0)\lambda_{th} D_b^2 c_p \rho} \qquad (2)$$

Then for $\theta_0 = 0.26$ rad (or 15°), $\overline{R} = 0.5$, $\lambda_{th} = 7.5\times10^{-5}$ cm, $D_b = 0.025$ cm, $c_p = 0.14$ J·g^{-1}·K^{-1}, and $\rho = 19.4$ g·cm^{-3} one obtains $\Delta T_{tip} \cong (1.8\times10^7 E_p)$ K or 18 K at $E_p = 1$ μJ. An energy up to 15 μJ was used in our experiments. This estimation is very

sensitive to the value of the θ_0. For example, for $\theta_0 = 30°$ the tip apex temperature rise is one-half as less, $\Delta T_{tip} \cong 9$ K at $E_p = 1$ μJ.

This coarse estimation, eqn. (2), is in a good agreement with the comprehensive 3D calculation due to Miskovsky *et al.*[17] A tungsten tip with a cone angle of 15° was "immersed in an azimuthally symmetric laser beam" which produces a surface heating power $Q = 1$ MW·cm^{-2} during the laser pulse of $\tau_{ref} = 30$ nsec. As was quoted above the temperature rise is proportional to the laser fluence. Therefore, taking into account the tungsten reflectivity, $\overline{R} = 0.5$, one can adjust the reported (ref. 17) tip apex temperature rise, ΔT_{ref}, to the conditions of our experiment:

$$\Delta T_{tip} \cong \Delta T_{ref} \frac{4E_p(1 - \overline{R})}{\pi D_b^2 Q \tau_{ref}} \qquad (3)$$

Taking $\Delta T_{ref} = 340$ K (ref. 17) one gets $\Delta T_{tip} \cong (1.2\times10^7 E_p)$ K or 12 K at $E_p = 1$ μJ which is close enough to the estimation determined from eqn. (2).

4.1.2 Tip Thermal Expansion

The agreement encourages us to use this simple model for the tip thermal expansion estimation. Figure 5 may be useful in order to understand a concept of the model which we employ to estimate the tip thermal expansion. First of all, an expansion of the λ_{th} - vicinity of the tip apex will have the strongest impact

on the tip-sample gap reduction induced by the laser. An expansion within the λ_{th} - thickness surface layer of the tip (Fig. 5) separated from the apex by several λ_{th} - lengths will not affect the gap reduction since its major expansion direction is virtually normal to the tip axis.[20] Therefore, the tip length which experiences the expansion may be estimated as:

$$h_{exp} \cong \eta\lambda_{th}, \qquad (4)$$

where η is the tip geometry factor in the range from 1 to 3 depending on the tip cone angle. Using (4), the tip-sample gap reduction caused by the tip thermal expansion can be estimated:

$$\Delta S_{tip} \cong \alpha h_{exp} \Delta T_{tip}, \qquad (5)$$

here α is the coefficient of linear thermal expansion. For tungsten $\alpha = 4.5\times10^{-6}$ K^{-1} (ref. 21). Assuming $\eta = 2$ and employing $\Delta T_{tip} = (1.2\times10^{7} E_p)$ K (eqn. 3) and λ_{th} = 7500 Å, one has:

$$\Delta S_{tip} \cong (8\times10^{5} E_p) \text{ Å or } 0.8 \text{ Å at } E_p = 1 \mu J. \qquad (6)$$

4.1.3 Nottigham Heating of Tip Due to Transient Current

In the following section we employ the experimental values of the current in order to estimate an additional tip heating effect induced by the transient tunneling current.

The following scenario is expected. The tip is heated by the laser pulse, giving $\Delta T_{tip} \cong (1.2\times10^{7} E_p)$ K. Then the tip expands toward the sample surface reducing the gap, giving $\Delta S_{tip} \cong (8\times10^{5} E_p)$ Å. Significant transient current flows between the tip and the surface. The tip expansion and, hence, the transient tunneling last for a time τ_p, or ~ 10^{-8} sec (refs. 16, 17). Therefore, the STM feedback with a response time of ~ 10^{-5} sec can be neglected.

The bulk resistivity heating of the tip by the pulse (~ 10^{-8} sec) current of ~ 10 μA is negligible.[3,17,22] Indeed, a transient temperature increase induced by the short pulse of current is:

$$\Delta T \cong \frac{J^2 \tau_p}{c_p \rho \sigma}, \qquad (7)$$

where J is the current density; c_p, ρ and σ are the heat capacity, the density and the conductivity of tungsten, respectively. Equation (7) indicates that in order to get a transient temperature rise of ~ 10 K during the 10^{-8} sec pulse one should pass 10 μA current through the tungsten ($\sigma = 1.79\times10^{5}\ \Omega^{-1}\cdot cm^{-1}$) wire with a radius of ~ 40 Å.

Based on the above analysis, the observed current pulse can resistively heat the tip apex of a few atoms only. This is, therefore, primarily a surface rather than a bulk heating. As was shown by Xu *et al.*[23] in such cases the total power delivered to the tip-sample junction, $W \cong IV$, is split into two approximately equal parts between emitter and receiver surfaces. Depending on

the transient current density and, hence, on the apex temperature, the power is supplied to the junction by resistive heating or through the Nottingham effect.[17,22,23] In any case the transient apex temperature can be estimated using the following equation (ref. 2):

$$K \frac{dT}{dr} 2\pi r_e^2 = \zeta IV \qquad (8)$$

or

$$\Delta T \cong \frac{\zeta IV}{2\pi K r_e}, \qquad (9)$$

where K is the thermal conductivity, $\zeta = 0.5$ is the fraction of the total power released on emitter (or receiver), and r_e is the mean free path for the electrons responsible for the energy transfer from the tip apex or from the vicinity of sample tunneling point, as shown schematicaly in Figure 5.

The energy is released in a small volume, $r_e \leq 100$ Å. The time of thermal diffusion, $\tau_{th} \sim r_e^2/\chi \sim 10^{-11}$ sec, is much less than the laser pulse duration, τ_p. Therefore, the apex heating is a quasi steady state process, and the ΔT follows the delivered power rather than the total energy, cf. eqn. (1).

As was shown by Flores *et al.*,[24] the energy transfer mechanism may be different for various tip-sample biases, V. Correspondingly, the values of r_e and K (the later is roughly proportional to r_e) may vary significantly with V. According to Flores *et al.*,[24] r_e may vary from 5 to 100 Å.

Let us estimate the top limit for the transient temperature of the tip apex accessible through this mechanism. For $I = 10^{-5}$ A, $V = 1.3$ V, $r_e = 5$ Å and $K_e \cong K/20 \cong 0.09$ W·cm^{-1}·K^{-1}, one gets the $\Delta T = 230$ K. Here K_e is the local thermal conductivity due to the special electron-hole pair energy transport[24] and K is the conventional tungsten thermal conductivity.[21] With an original laser heating of ~ 120 K ($E_p = 10$ μJ), obtained from eqn. (3), the total transient temperature rise is ~ 350 K and, hence, the local transient tip apex temperature, T_{tip}, may reach as high as ~ 650 K.

The above estimations are related to the extremely small volume of few tungsten atoms. Therefore, the temperature is proportional to the vibrational energy of single atom averaged in time rather than over ensemble of these few atoms at certain a moment.

The apex atom (atoms) behavior may be strongly affected by the arrival of the hot electrons responsible for the tunneling current. The current of 10^{-5} A corresponds to a single electron tunneling transfer time of ~ 1.6×10^{-14} sec. This time is much longer than the time necessary for the electron escape from the region of the apex of radius r_e (~ 10^{-15}-10^{-16} sec). A direct energy transfer from the hot electron to the phonons is substantially less probable.[25] Therefore, the estimation (9) which assumes, following ref. 24, that the hot electron-hole pair energy transfer to the electron gas followed by the electron-phonon relaxation is most likely correct.

4.1.4 *Sample Surface Heating and Thermal Expansion*

To estimate the silicon surface temperature rise induced by the laser one can use a simple and reliable expression[16]:

$$\Delta T_s \cong \frac{4E_p(1-\overline{R})\cos\theta_i}{\pi D_b^2 c_p^{Si}\rho^{Si}\lambda_{th}^{Si}}, \qquad (10)$$

where θ_i is the laser incident angle (Fig. 5); c_p^{Si} and ρ^{Si} are the silicon heat capacity and density, respectively; λ_{th}^{Si} is the thermal diffusion length estimated for silicon (χ = 0.9 cm^2s^{-1}) as ~ $(\chi\tau_p)^{1/2} \cong 8500$ Å; $\overline{R}$ is the silicon reflectivity for the laser of 532 nm at the θ_i.

Taking θ_i = 80°, $\overline{R}$ = 0.7, D_b = 0.025 cm, c_p^{Si} = 0.71 $J\cdot g^{-1}\cdot K^{-1}$, and ρ^{Si} = 2.33 $g\cdot cm^{-3}$ one obtains $\Delta T_s \cong (0.75\times10^6\ E_p)$ K. This is much less than the ΔT_{tip} (see eqns. 2 or 3). Using equation (5), η =1 and α = 3.8×10^{-6} K^{-1} (ref. 21), the silicon surface thermal expansion can be estimated now as $\Delta S_s \cong (2.4\times10^4\ E_p)$ Å or 0.024 Å at E_p = 1 μJ.

Since $\Delta S_s << \Delta S_{tip}$ and $\Delta T_s << \Delta T_{tip}$, one may exclude the laser induced sample heating and the sample thermal expansion from consideration.

4.2 *Transient Tunneling of Non-Thermal Electrons*

The enhancement of the tunneling current during the laser pulse is due, at least in part, to the thermal expansion of the tip toward the surface. There are,

however, other mechanisms involving the direct excitation of electrons which might also contribute to the transient tunneling current. These mechanisms involve photo induced tunneling of hot electrons from the tip or from the silicon sample depending on the bias voltage applied. Two mechanisms can be imagined:

(1) Tunneling of hot electrons before their relaxation to the bottom of the conductor band (tip and sample).

(2) Tunneling of non-equilibrium electrons thermalized at the bottom of the conduction band (sample) and captured in a potential well induced by the tip.

The symmetry of the laser induced tunneling current versus bias voltage dependence (Fig. 2) argues against the role of ballistic tunneling of high energy electrons since the metal tip and the silicon have dissimilar electronic properties.

Finally, the magnitude of the experimentally observed transient tunneling current is larger than can be explained by mechanisms (1) and (2) above. The two hot electron tunneling mechanisms are discussed in detail in the Appendix to this paper.

4.3 Mechanism of Transient Electron Tunneling

At the highest laser pulse energies used in our charge transfer experiments (2.4 μJ) one might expect the tip temperature to be increased ~ 330 K. From eqn. (6), for 2.4 μJ, pulses, $\Delta S_{tip} \cong 1.9$ Å.

The linear dependence of the transient tunneling current on laser pulse energy argues that tip expansion cannot be the entire cause of the enhanced tunneling current; the transient current should depend exponentially on the ΔS_{tip} and, hence, on the laser pulse energy, E_p, as shown in eqn. (11) (ref. 2):

$$I_p \equiv I_{ref} \exp\left(2\Delta S_{tip}\sqrt{\frac{2m}{\hbar^2}\left(\overline{\Phi} - \frac{|qV|}{2}\right)}\right), \qquad (11)$$

where I_p and I_{ref} are the transient and reference tunneling currents, m is an electron mass; q is an electron charge; $\hbar$ is the Planck constant divided by 2π; V is the sample bias potential; $\overline{\Phi} = \frac{\Phi_{tip} + \Phi_s}{2}$, where Φ_{tip} and Φ_s are tip and sample work functions, respectively.

Furthermore, eqn. (11) indicates that a maximum transient current would be observed at zero tip-sample bias, in contrast to the experiments where the current maximum is at ~ ± 3V bias. Thus additional factors beyond tip expansion must be at work in these experiments.

4.4 Mechanism of Atom Transfer From Tip to Sample

Considering the heating of the tip by the laser, eqn. (3), and by the Nottingham heating (Section 4.1.3), a maximum tip temperature of 650 K may be estimated, using a laser pulse energy of ~ 10 μJ and observing a transient electron

current of 10 μA. Can this temperature lead to the evaporation of an apex W atom?

Several approaches indicate that the binding of W will be considerably diminished from its bulk value of 8.9 eV/atom for an apex W atom as outlined below:

(1) For the Debye frequency of W of ~ 8×10^{12} sec^{-1} (ref. 25), and a pulse duration of 8×10^{-9} sec, the desorption of a single atom at 650 K corresponds to an activation energy of ~ 0.6 eV.

(2) Below ~ 100 Å particle diameter, the binding energy is a strong function of the particle size.[26] For example, the melting temperature of Au is 1/4 of its bulk value at a particle diameter of 25 Å.

In addition, the tip apex atom transfer occurs readily at both polarities of tip-sample bias voltage, and the laser energy thresholds of atom transfer are similar for both polarities. This result rules out the importance of a field effect on the atom transfer in our case.[27]

Finally, an additional reduction in activation energy for laser desorption of a tip W atom is expected from the interaction with the Si surface, as suggested by Lyo and Avouris.[28] As the tip-sample gap is decreased, the apex W atom may chemically interact with surface Si atoms as it begins to transfer, collapsing the activation energy to a low value.

5. *Summary*

Nanosecond laser pulses, with 2.33 eV photon energy and ~ 0.6 MW/cm^2 radiation flux, have been used to initiate a transient increase of tunneling current between tip and sample surface in an ultrahigh vacuum STM apparatus. In addition, at higher laser power, single atom transfer from the tip to the silicon sample occurs. The following conclusions may be made:

(1) The laser induced tunneling current is linear with laser pulse flux up to ~ 0.6 MW/cm^2, independent of the sign of the tip-surface bias, Figure 1(a) and 1(b).

(2) At constant laser pulse energy, the transient tunneling current exhibits a complex dependence on the tip-sample bias (Figure 2). The similarity of the laser induced tunneling for both bias conditions suggests that the tunneling mechanism is the same in both directions, independent of the material of the electron emitter.

(3) At a laser pulse flux of ~ 2.5 MW/cm^2, single atom transfer occurs between the tip and the Si sample by a process virtually independent of the bias polarity. The number of transferred atoms per pulse can be controlled by the laser energy.

(4) The dominant laser induced electron tunneling and atom transfer effects are proposed to be due to pulse laser heating of the tip, causing nanosecond thermal expansion and a decrease in the tunneling gap. Additional heating

may occur as a result of Nottingham heating at the high transient tunneling currents.

(5) Estimates have been made of a maximum temperature of 650 K for the tip due to light absorption and the Nottingham heating. The transfer of a W atom from the tip to the sample is postulated to occur at such low temperatures as a result of both the low coordination number of an apex W atom (compared to the bulk), leading to a low W atom binding energy, and to the proximity of the Si surface leading to strong chemical interaction with the surface W atom as it transfers.

(6) W atom transfer occurs without significant damage to the tip, as it continues to provide STM images. In addition, damage to the silicon surface also does not occur.

(7) W atom transfer induced by the pulse laser is fast (~ 8 nsec) in comparison to slow transfer processes involving the pulsing of piezodrive devices (~ 100 μsec). This is due to their inertia, and their electronic and acoustical ringing.

(8) Ballistic electron tunneling at a laser flux of ~ 1 MW/cm^2 has been rejected on the basis of estimations contained in Appendix A.

(9) Surface band bending compensation induced in silicon by high transient current is ignored in our discussion. In both tunneling directions such effects may exist and contribute to the current-voltage relationship. Surface band bending compensation may be responsible for the linear relationship between

transient tunneling current and laser power, Figure 1(a) and 1(b), where a non-linear relationship is expected if tip expansion were solely involved.

Acknowledgments

The authors gratefully acknowledge the full support of the Office of Naval Research. We wish to express our appreciation to Robert J. Muha for modeling and numerical simulation of the transient processes of the STM electronics. We also want to thank Z. Dohnalek for his help and stimulating discussions.

Figure Captions

Figure 1. Dependence of the laser induced transient tunneling (LITT) current on laser flux: (a) positive (1.3 V) sample bias; (b) negative (-1.3 V) sample bias. Laser flux calculated for sample surface.

Figure 2. Dependence of the laser induced transient tunneling current on tip-sample bias voltage. Constant laser flux of ~ 0.6 MW/cm^2 or laser pulse energy of 2.4 μJ.

Figure 3. Illustration of the laser induced single atom transfer. Laser flux ~ 3 MW/cm^2. Sample bias: -1.3 V. (a) STM image of Si(001)-(2x1) before the transfer. (b) STM image of Si(001)-(2x1) during the transfer. (c) STM image of Si(001)-(2x1) with the six single tip atoms deposited by the six laser pulses.

Figure 4. Cross-section of the STM image of the six single atoms deposited by six laser pulses (see also Fig. 3). Sample bias voltage: -1.3 V. Reference tunneling current: 1 nA.

Figure 5. A schematic presentation of the STM tip-sample junction irradiated by a laser. Here θ_i is the laser incident angle, D_b is the laser beam diameter, θ_0 is the tip cone angle, w is the maximum radius of the tip cone irradiated by the laser, r_t is the tip radius, r_e is the mean free path for electrons responsible for the energy transfer, λ_{th} is the thermal diffusion length during the 8 nsec laser pulse.

Figure 6. An energy diagram of the STM junction between p-type Si(001)-(2x1) and a metal tip. Empty and occupied surface electronic bands shown as π^* and π, respectively. (a) Zero sample bias voltage. No laser. (b) Negative sample bias voltage. No laser. (c) Negative sample bias voltage. Laser is on.

Appendix A. Transient Tunneling of Non-Thermal Electrons

An alternative explanation for the transient tunneling current is the photo induced tunneling of non-thermal or "hot" electrons. This phenomenon has been briefly discussed by McEllistrem *et al.*[4] and, finally, neglected in the case of "moderate illumination intensities" (5 mW, CW laser). A laser power density up to 4 MW/cm^2 has been used in our experiments and, hence, the direct tunneling of photo induced carriers should be reconsidered.

Energy diagrams for the normal and the photo induced tunneling from the p-type Si(001)-(2x1) to the metal tip (at negative sample bias) are presented in Figures 6(a),(b) and (c). According to Chahill and Hamers,[29] tunneling currents of ~ 1 nA should considerably charge the semiconductor surface under the tip and induce significant band bending is shown in Figure 6(b). For a high resistivity semiconductor (100 Ω·cm) this effect may be much higher than the band bending induced by the electrostatic field of the tip.[4,29]

The energy distribution of the photo excited carriers in a semiconductor experiences a complicated evolution in time and is affected by the presence of various defects, for example, by a surface.[30,31,32] The photon absorption in silicon occurs in a large penetration depth of ~ 10^4 Å (532 nm, 2.33 eV). The photo excited electrons form the Boltzmann distribution in the conduction band of Si(001)-(2x1) in less than 120 fsec. An effective "temperature" of these excited conduction band electrons is much higher than the lattice temperature. It takes

about 1 psec to reduce this electron "temperature" down to the lattice temperature.

About the same time, ~ 1 psec, is necessary to form so called Surface Charge Layer (SCL).[30,31,32] The SCL is a transient surface charging due to the photo excited carriers separation in the electrostatic field of the semiconductor surface or any other defect. The STM tip, biased with respect to the sample, may be considered as a such "defect." The mechanism of the transient charging should be similar for a surface and for any other defect.

As shown by Long *et al.*[32] the lifetime of the non-equilibrium carriers in the vicinity of the defect may reach several μsec. The reason for this slow recombination is a spatial separation of the photo excited electrons and holes.

As a result of this complex process the photo induced tunneling current has two components. One is the current due to the tunneling of the photo excited electrons before their relaxation down to the bottom of the conduction band. The second component is related to the tunneling of the CBM or the non-equilibrium electrons thermalized on the bottom of the conduction band and trapped in the vicinity of the tip. These two possibilities are discussed in sections A.1 and A.2 below.

A.1 Ballistic Tunneling of High Energy Photo Electrons from Silicon and Metal

The high energy non-thermalized photo electrons have a vanishing chance to tunnel toward the tip simply because of their short life time (less than 10^{-13} sec) and extremely low probability to hit the surface right under the tip (the band bending is not enough to guide the high energy electrons toward the tip).

Indeed, the fluence of absorbed photons by the sample is:

$$F_p \cong \frac{4E_p(1-\bar{R})\cos\theta_i}{\pi D_b^2 h\nu}, \qquad \text{(A-1)}$$

where $h\nu$ is the laser photon energy (2.33 eV). This is ~ $(2.8\times10^{20}\ E_p)$ ph/cm^2. Here and below the units of E_p are Joules.

Considering the photon absorption length, λ_{abs}, and the life time of the non-thermalized electrons, τ_{he}, the density of such electrons in the absorption layer can be estimated as:

$$n_{he} \cong \frac{F_p\tau_{he}}{\lambda_{abs}\tau_p}. \qquad \text{(A-2)}$$

Then taking into account the speed of the electrons, V_e; the effective area of tunneling, A; and the tunneling probability, P; one gets for the tunneling current of the high energy electrons:

$$I_{he} \le \frac{F_p\tau_{he}}{\lambda_{abs}\tau_p} AqV_eP. \qquad \text{(A-3)}$$

For $\tau_{he} = 10^{-13}$ sec, $A = 10^{-14}$ cm^2, $q = 1.6\times10^{-19}$ C, $V_e = 10^8$ cm/sec, $P = 10^{-4}$, and $\lambda_{abs} = 10^{-4}$ cm, one obtains: $I_{he} \leq (6\times10^{-10}\ E_p)$ A. For the laser energies used in our experiments, $E_p \leq 15$ μJ, the calculated value of I_{he} is less than 10^{-14} A and, hence, may be neglected.

The above consideration and eqns. (A-1 to A-3) can be applied for the I_{he} estimation in the case of electron tunneling from the metal tip to the semiconductor as well. Using for tungsten $\overline{R} = 0.5$, $\theta_i = 0°$, $\tau_{he} = 10^{-13}$ sec, and $\lambda_{abs} = 10^{-6}$ cm, one has: $I_{he} \leq (6\times10^{-7}\ E_p)$ A and, hence, in our experiments the I_{he} is less than 10^{-11} A and should be neglected also.

A.2 Photo Electron Tunneling from Bottom of Silicon Conduction Band

As soon as the photo excited electrons are thermalized on the bottom of the semiconductor conduction band they are driven by the electric field toward the surface and the tip. Finally, they are trapped in the SCL and in the tip vicinity and recombine during several μsec. Three major processes serve as a sink for these trapped electrons: (i) the tunneling from the conduction band of the sample to the tip, (ii) the thermal current of majority carriers (holes) to the surface,[29,33] and (iii) the tunneling from the valence band to the tip. The two later processes are accompanied by surface electron-hole recombination.

The CBM electron trapping in the tip vicinity reduces the band bending and, hence, is self-limiting. As we will show below, the quasi steady state

tunneling current should depend, mainly, on the initial (prior to the laser pulse) band bending, the initial majority carrier density, the density of photo excited electrons and the tunneling probability.

This process is complex and, to the best of our knowledge, is not understood and described yet. There was an attempt to apply the Schottky barrier theory to the case of a low intensity laser irradiation of the tip-semiconductor junction.[29] Few other analytical and numerical attempts (refs. 34, 31, 32) have been made to solve the problem of the SCL formation and its evolution (in absence of the tip) under the nanosecond pulse laser with intensity up to ~ 10^5 W/cm^2.

A comprehensive numerical simulation, probably, might (see, for example, ref. 32) solve the problem but this is beyond the scope of this publication. Instead, we suggest a simple model which is in reasonable agreement with the experimental data obtained for the one-dimensional (the SCL) case.[32,30] This model is designated to provide order of magnitude estimations for the case of pulse laser irradiation of the tip-semiconductor junction.

The density of the photo electrons under the tip is a crucial parameter for the laser induced tunneling current estimation. Since the characteristic surface recombination time of the non-equilibrium carriers is longer than the laser

pulse,[32] the density of the CBM electrons in the absorption layer can be estimated as:

$$n_{cb} \cong \frac{F_p}{\lambda_{abs}}. \qquad \text{(A-4)}$$

Taking $\lambda_{abs} = 10^{-4}$ cm, one has ~ $(3\times10^{24}\ E_p)$ cm^{-3} for the non-equilibrium carriers density. At laser energy of $E_p = 1$ μJ the n_{cb} equals 3×10^{18} cm^{-3}.

This value is much higher than the initial density of carriers in the 100 Ω·cm p-type silicon crystal at 300 K. Using the hole mobility in silicon, $\mu_p = 500$ cm^2/V·sec (ref. 21), one gets the density of majority carriers, $p = 1.25\times10^{14}$ cm^{-3}. The corresponding Debye length, λ_D, and, hence, the depth of the initial surface band bending is estimated as ~ 2600 Å.

The density of photocurrent headed for the SCL can be computed as (ref. 33):

$$J_{pc} = J_{pc0}\left(1 - e^{-\frac{\lambda_D}{\lambda_{abs}}}\right), \qquad \text{(A-5)}$$

where $J_{pc0} = \frac{qF_p}{\tau_p}$.

To adjust this formula to the tip-surface 3D case, one can simply assume a collection of the CBM electrons within the range λ_D from the tip. Therefore, for the density of the photocurrent toward the tip one gets:

$$J_{pc}^{tip} = \frac{J_{pc0}\pi\lambda_D^2}{A}\left(1 - e^{-\frac{\lambda_D}{\lambda_{abs}}}\right), \qquad \text{(A-6)}$$

here A is the effective area of tunneling. Thus, taking $A = 10^{-14}$ cm^2 and $T = 300$ K, one obtains the top limit estimation for the photocurrent under the tip: $J_{pc}^{tip} \leq (2.7\times10^{14}\ E_p)$ A/cm^2 (ref. 35).

The CBM photo electrons driven by the electrostatic field should hit the surface under the tip. Therefore, the flux of these electrons on the surface and their effective density under the tip can be estimated as:

$$F_{pc}^{tip} = \frac{J_{pc}^{tip}}{q} = n_{cb}^{tip}\frac{V_{th}}{4}, \qquad \text{(A-7)}$$

where V_{th} is a thermal speed of an electron at 300 K (~ 10^7 cm/sec). Equation (A-7) gives an estimation for the effective density of the CBM photo electrons: $n_{cb}^{tip} \leq (7\times10^{26}\ E_p)$ cm^{-3}. At laser energy of $E_p = 1$ μJ the $n_{cb} \leq 7\times10^{20}$ cm^{-3}. The number is ~ 2 orders of magnitude higher than the bulk density of the CBM photo electrons estimated by eqn. (A-4).

This value is of the same order of magnitude as the surface density of the CBM electrons in the SCL obtained for Si(001) and for Si(111) by Long *et al.*[32] and by Goldman and Prybyla,[30] respectively. Laser fluences of ~ 100 μJ/cm^2 ($h\nu$ = 2.43 eV) and of ~ 250 μJ/cm^2 ($h\nu$ = 2 eV) have been used in these experiments.

An incident laser fluence of ~ $0.35\times10^{6}\ E_p$ mJ/cm^2 ($h\nu$ = 2.33 eV) has been employed in our experiments (no correction for reflection is made).

Using the J_{pc}^{tip}, eqn. (A-6), one can compare now the photo induced and the reference tunneling currents. Assuming that the tip thermal expansion influences both currents equally, we compare them at zero tip expansion. The density of the reference tunneling current is in the range of (10^5-10^6) A/cm^2 at a current of 1 nA. The corresponding effective current density in the semiconductor under the tip should be significantly higher, ~ (10^9-10^{11}) A/cm^2, due to low value of the tunneling probability, ~ (10^{-4}-10^{-5}).

In conclusion, the photocurrent density under the tip, eqn. (A-6), may reach the low limit of the reference current density, 10^9 A/cm^2, at relatively high laser energy of ~ 4 μJ (cf. Figs. 1 and 2). Thus, the tunneling of the CBM electrons may be neglected in our studies of the laser induced tunneling but, probably, plays a minor role in the laser induced atom transfer process (Figs. 3 and 4).

In the light of these estimations, it is not surprising that the STM reference current has a pronounced influence on the Surface Photo Voltage (SPV) measurements at moderate laser intensities.[29]

Appendix B. STM Tip as Conical Antenna

Here we examine the possibility that the tip can work as a conical antenna or in other words as a wave guide for the laser.[3] The narrowing of the tip-surface gap toward the point of tunneling may operate as a wave guide as well.[36]

Following Sullivan *et al.*[3] one may expect an electrical field magnification by the factor of ~ w/r_t, where w is the maximum radius of the tip cone irradiated by laser (Fig. 5) and r_t is the tip radius. Since in our case $w \cong 30$ μm which is much greater than the laser wavelength, $\lambda = 0.532$ μm, the field enhancement factor should be rather estimated as λ/r_t or as ~ (5-50). A value of r_t ~ (100-1000) Å has been used in this order of magnitude estimation.

The laser intensity is proportional to a square of the field and, hence, the corresponding gain in the photon flux may be expected to be as high as ~ (25-2500). If the above estimations are correct, one would expect to have a laser flux in the tip-sample junction of ~ (10^{13}-10^{15} E_p) W/cm^2. At the highest $E_p = 15$ μJ it should be ~ (10^8-10^{10}) W/cm^2. Such a high laser flux would be enough to initiate extensive metal and silicon evaporation followed by plasma formation at the tip-sample junction.[16]

To get any appreciable transient current of the high energy photo electrons from the metal tip (cf. eqn. (A-3) and Fig. 2), a laser flux under the tip should be increased by a factor of ~ (10^6-10^7) with respect to the one calculated by

eqn. (A-1). Thus, at the tip apex one would need a laser flux of ~ (10^{16}-10^{17} E_p) W/cm^2. Such a high flux must create a plasma above the metal surface.

A laser induced plasma would be expected to cause severe acoustical noise,[16] and widespread damage of the Si(001) surface. Neither of these signs are seen experimentally.

Nevertheless, one can not exclude a laser intensity gain less than a factor of 25, which could intensify significantly the laser heating and the thermal tip expansion as well as the tunneling of the CBM photo electrons from the semiconductor surface. This problem requires further investigation.

References

[1] M. Ringger, H. R. Hidber, R. Schögl, P. Oelhafen and H.-J. Güntherodt, Appl. Phys. Lett. 46 (1985) 832.

[2] R. Wiesendanger, *Scanning Probe Microscopy and Spectroscopy. Methods and Applications.* (Cambridge University Press, Cambridge, GB, 1994).

[3] T. E. Sullivan and P. H. Cutler and A. A. Lucas, Surf. Sci. 62 (1977) 455 and references therein.

[4] M. McEllistrem, G. Haase, D. Chen, and R. J. Hamers, Phys. Rev. Lett. 70 (1993) 2471.

[5] R. J. Hamers and K. Market, Phys. Rev. Lett., 64 (1990) 1051; Y. Kuk, R. S. Becker, P.J. Silverman, and G. P. Kochanski, Phys. Rev. Lett. 65 (1990) 456.

[6] S.-T. Yau, D. Saltz, and M. H. Nayfeh, Appl. Phys. Lett. 57 (1990) 2913; J. Vac. Sci. Technol. B9 (1991) 1371.

[7] L. L. Kazmerski, J. Vac. Sci. Technol. B9 (1991) 1549; Vacuum 43 (1992) 1011.

[8] C.-Y. Liu and A. J. Bard, Chem. Phys. Lett. 174 (1990) 162.

[9] E. Betzig, J. K. Trautman, R. Wolfe, E. M. Gyorgy, P. L. Finn, M. H. Kryder, and C.-H. Chang, Appl. Phys. Lett. 61 (1992) 142.

[10] H. J. Mamin and D. Rugar, Appl. Phys. Lett. 61 (1992) 1003.

[11] S. Hoen, H. J. Mamin, and D. Rugar, Appl. Phys. Lett. 64 (1994) 267.

[12] S. A. Mitchell and P. A. Hackett, J. Chem. Phys. 79 (1983) 4815.

[13] V. A. Ukraintsev and J. T. Yates, Jr., Surf. Sci. (in press).

[14] This 50 % discrepancy is mostly a systematic overestimation of the transfered charge which has no significant impact on the conclusions of the study.

[15] Another feature, a local minimum in the transient current exists at positive sample bias of ~ 0.5 V. This local minimum is not seen in Figure 2 which shows accumulative data averaged over different tip conditions and various surface sites (long, more than 2 hrs., data collection). The presence of the minimum is apparent with a rapid scan (~ 5-10 sec) over limited positive sample biases (for instance, from 0.1 to 0.7 V). The data are not presented.

[16] John F. Ready, *Effects of High-Power Laser Radiation* (Academic Press, N.Y.-London, 1971), Chapter 3.

[17] N. M. Miskovsky, S. H. Park, J. He, and P. H. Cutler, J. Vac. Sci. Techol. B11 (1993) 366.

[18] The volume of the λ_{th} vicinity of the tip apex is calculated as: $V_{th} = \frac{\lambda_{th}^3}{3}\Omega$, where Ω is the tip cone solid angle.

[19] This estimation of the absorbed laser energy is a crude approximation. The size of the tip apex is comparable with the laser wavelength of 5320 Å. Therefore, macroscopic or geometrical optics is not applicable to the case anymore. The laser energy absorbed by the tip should be calculated then by using the theory of light scattering and with knowledge of the exact geometry of the tip-surface junction (see, for example, C. F. Bohren and D. R. Huffman, *Absorption and scattering of the light by small particles*, Wiley, N.Y., 1983 or M. Born and E. Wolf,

Principles of Optics, 4th ed., Pergamon Press, N.Y., 1968). Moreover, the situation may be complicated by the surface polariton generation and various waveguide effects (see, for example, *Surface Polaritons*, edited by V. M. Agranovich and D. L. Mills, Elsevier, Amsterdam, 1982). To the best of our knowledge this complex problem has not been solved. At the present moment we restrict ourselves by this simplified approach which we believe still gives a correct order of magnitude estimation. The the possible laser intensity increase in the tip-sample junction are considered in Appendix B.

[20] The situation is similar to a one-dimensional thermal expansion of an infinite surface layer.

[21] *CRC Handbook of Chemistry and Physics*, 69th Edition, Ed. R. C. Weast, CRC Press, Boca Raton, 1989.

[22] S. I. Shkuratov, S. A. Barengolts, and E. A. Litvinov, J. Vac. Sci. Technol. B13 (1995) 1960.

[23] J. B. Xu, K. Läuger, R. Möller, K. Dransfeld, I. H. Wilson, Appl. Phys. A59 (1994) 155; J. B. Xu, K. Läuger, R. Möller, K. Dransfeld and C. C. Williams, in *Nanosources and Manipulation of Atoms Under High Fields and Temperatures: Applications*, edited by V. T. Binh *et al.*, Kluwer Academic Publishers, Netherlands, 1993, p. 89.

[24] F. Flores, P. M. Echenique, and R. H. Ritchie, Phys. Rev. B 34 (1986) 2899.

[25] Charles Kittel, *Introduction to Solid State Physics* (John Wiley & Sons, N.Y., 1986) Ch. 6.

[26] Ph. Buffat and J-P. Borel, Phys. Rev. A 13 (1976) 2287; T. Castro, R. Reifenberger, E. Choi and R. P. Andres, Surf. Sci. 234 (1990) 43.

[27] T. T. Tsong, Phys. Rev. B 44 (1991) 13703; N. M. Miskovsky, T. T. Tsong and C. M. Wei, in *Nanosources and Manipulation of Atoms Under High Fields and Temperatures: Applications*, edited by V. T. Binh *et al.*, Kluwer Academic Publishers, Netherlands, 1993, p. 207; N. D. Lang, *ibid.*, p. 177.

[28] I-W. Lyo and Ph. Avouris, Science 253 (1991) 173.

[29] D. G. Cahill and R. J. Hamers, J. Vac. Sci. Technol. B9 (1991) 564.

[30] J. R. Goldman and J. A. Prybyla, Phys. Rev. Lett. 72 (1994) 1364; Semicond. Sci. Technol. 9(1994) 694.

[31] N. J. Halas and J. Bokor, Phys. Rev. Lett. 62 (1989) 1679.

[32] J. P. Long, H. R. Sadeghi, J. C. Rife, and M. N. Kabler, Phys. Rev. Lett. 64 (1990) 1158.

[33] M. H. Hecht, J. Vac. Sci. Technol. B8 (1990) 1018.

[34] E. O. Johnson, Phys. Rev. 111 (1958) 153.

[35] One would expect a reduction of the λ_D and the λ_{abs} at higher density of the photo electrons. Indeed, at the high $n_{cb} = p_{vb} = 10^{21}$ cm^{-3}, the absorption length, $\lambda_{abs} \equiv \frac{c}{\omega_p} \sim 1600$ Å, is much higher than the corresponding Debye length, λ_D

~ 1 Å and, hence, the photocurrent should be dramatically reduced (*Physical Kinetics*, E. M. Lifshitz and L. P. Pitaevskii, Elsevier, Amsterdam, 1979, Chapter 9). Nevertheless, the high initial photocurrent, evidently (ref. 25), plays a crucial role in the SCL formation and pumps the surface electron density to this high value.

[36] A. Harootunian, E. Betzig, M. Isaacson, and A. Lewis, Appl. Phys. Lett. 49 (1986) 674; E. Betzig, M. Isaacson, and A. Lewis, Appl. Phys. Lett. 51 (1987) 2088; J. A. Cline, H. Barshatzky, and M. Isaacson, Ultramicroscopy 38 (1991) 299.

Dependence of LITT Current on Photon Flux

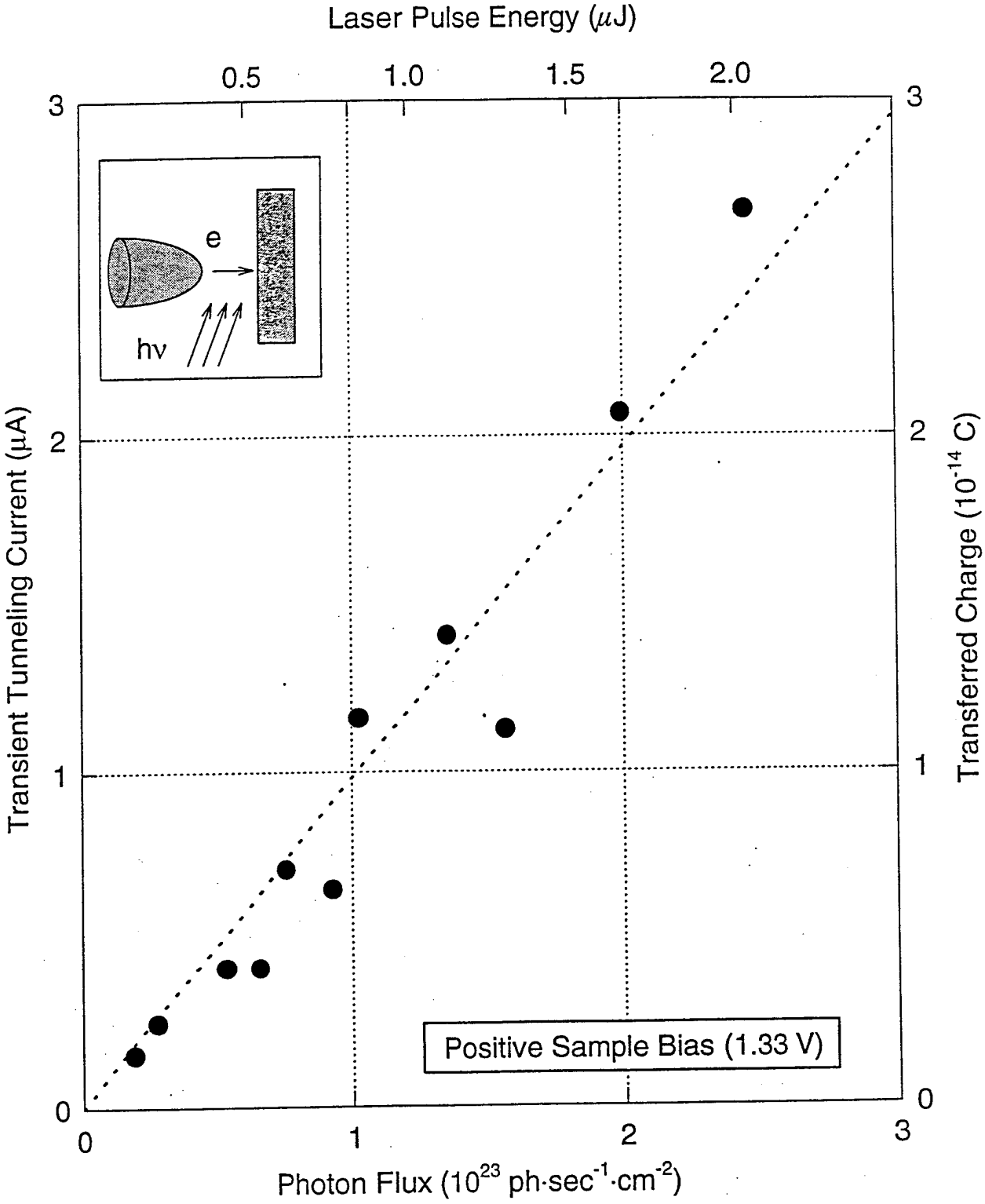

Figure 1(a)
Ukraintsev & Yates

Dependence of LITT Current on Photon Flux

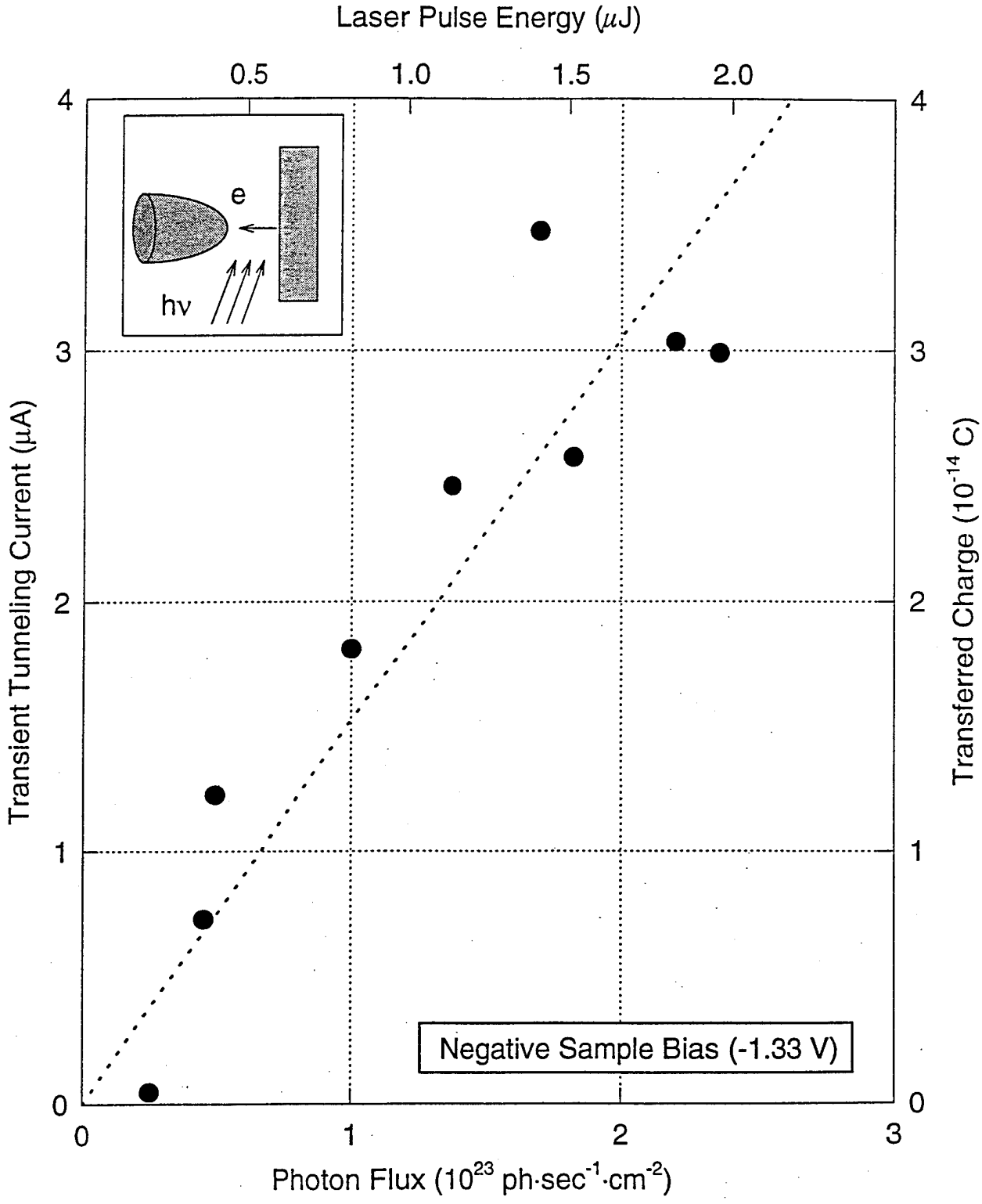

Figure 1(b)

Ukraintsev & Yates

Dependence of LITT Current on Sample Bias Voltage

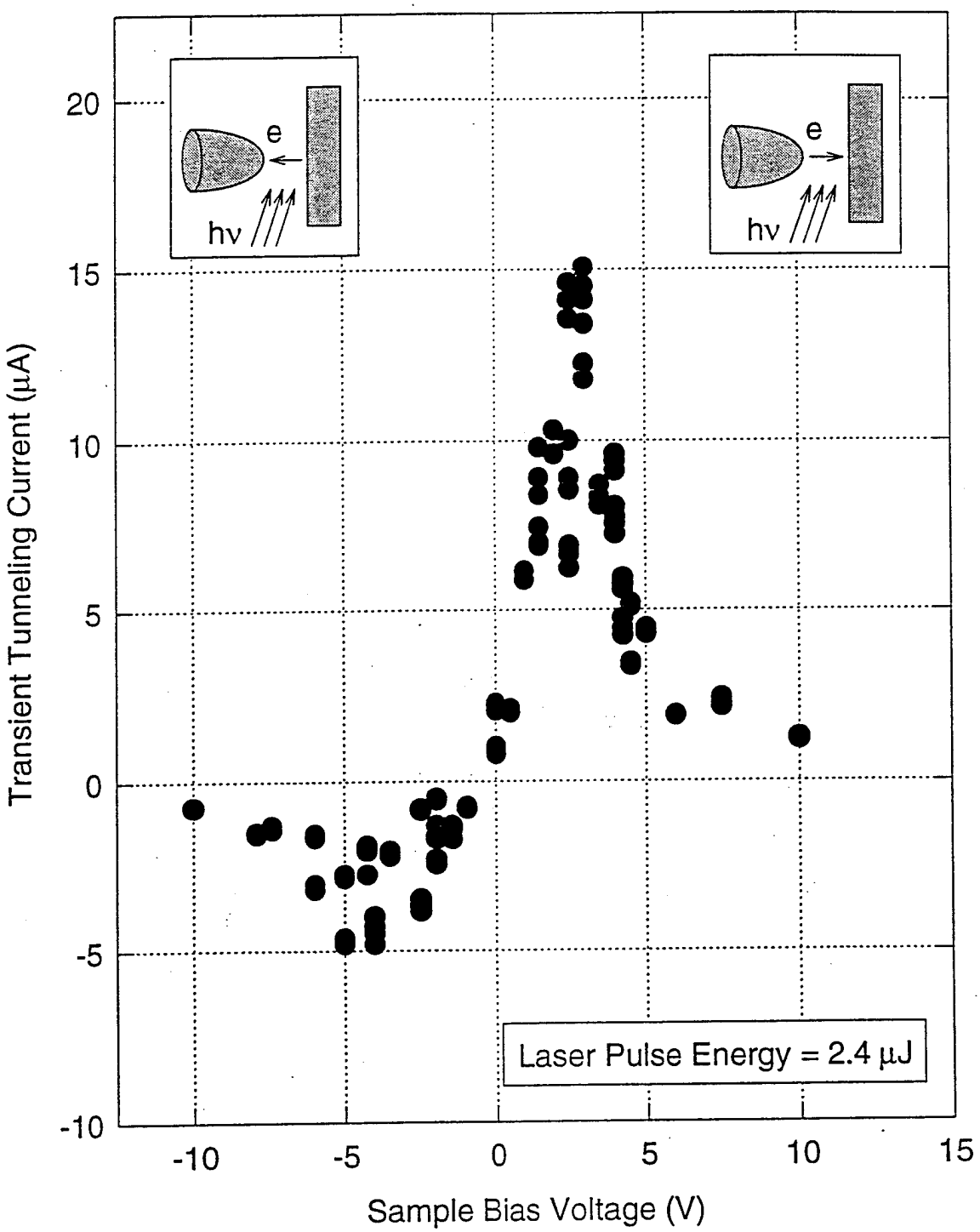

Figure 2
Ukraintsev & Yates

Laser Induced Single Atom Transfer

STM Image of Si(001)-(2x1) Before Laser Pulse Sequence

(a)

STM Image of Si(001)-(2x1) During Laser Pulse Sequence

(b)

STM Image of Si(001)-(2x1) After Laser Pulse Sequence

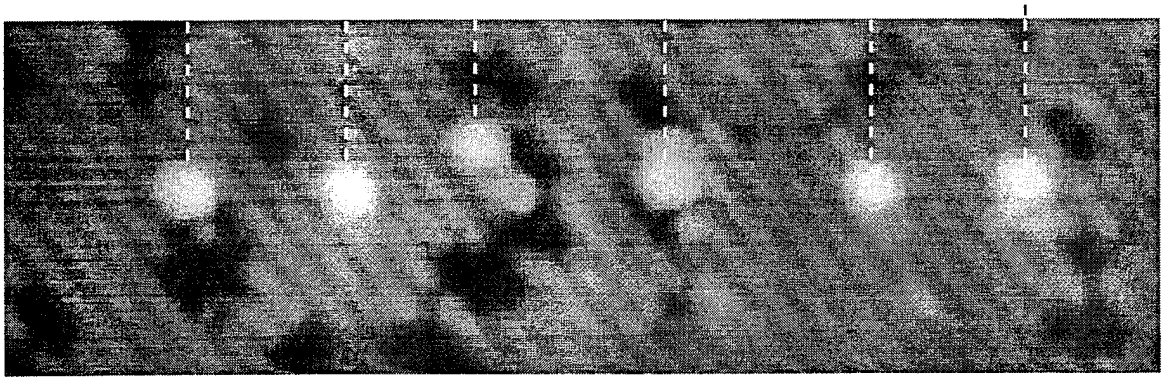

(c)

50 Å

Figure 3
Ukraintsev & Yates

Cross-Section of Atomic Periodic Structure Created by Sequence of Six Laser Pulses

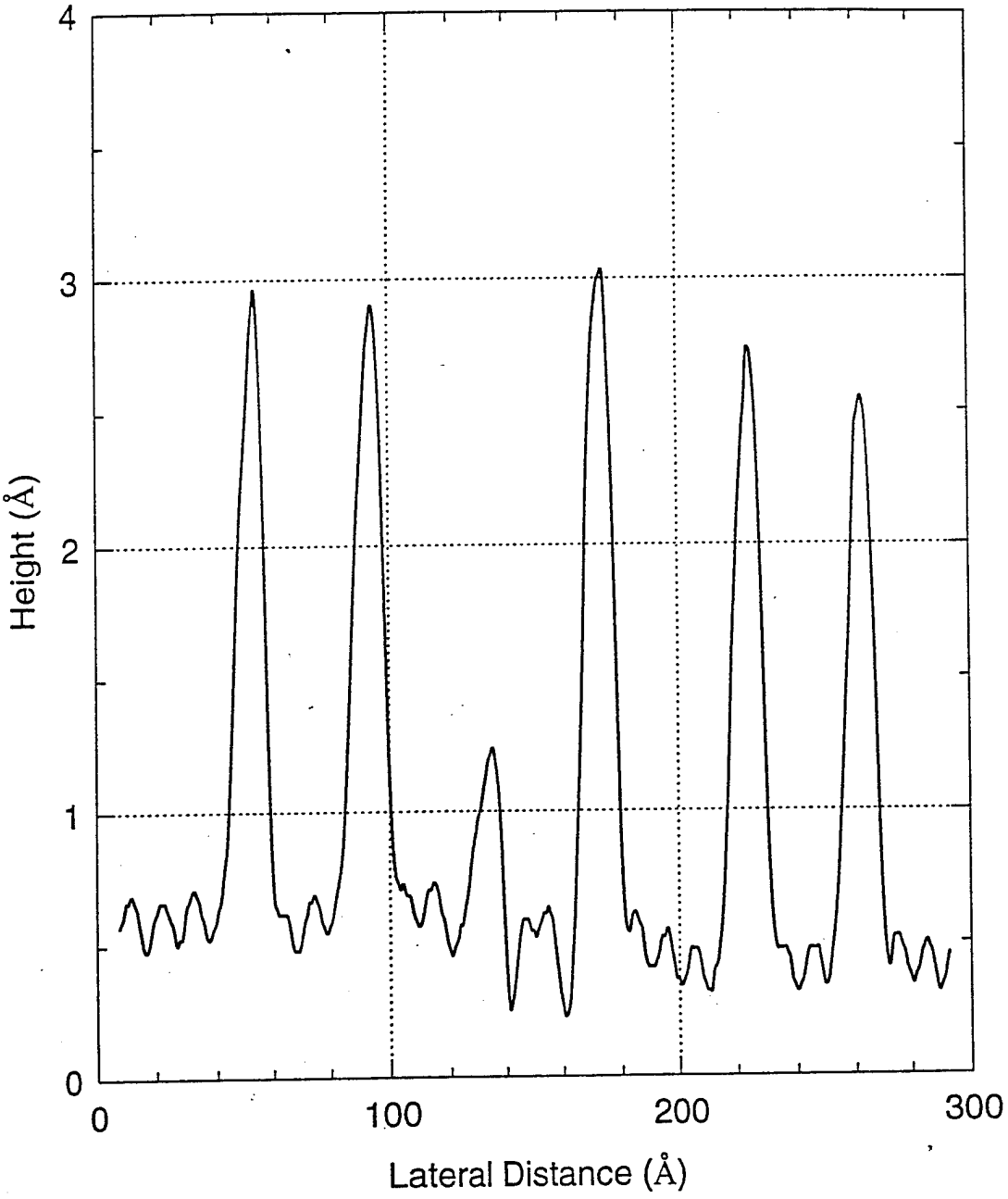

Figure 4

c:/vladimir/papers/nanofabrication/figures/fig4.spw

Ukraintsev & Yates

Pulse Laser Heating of STM Tip-Sample Junction

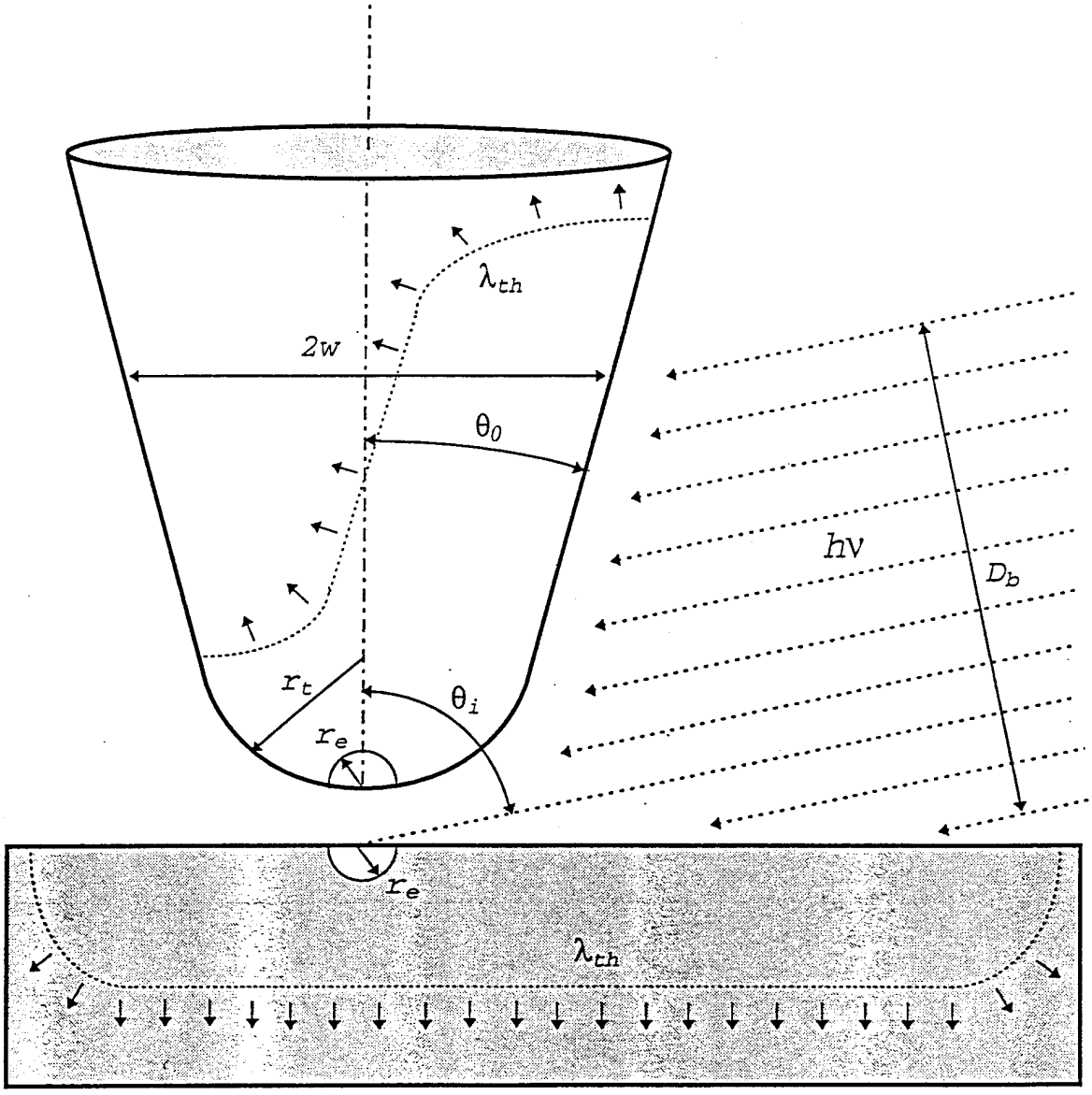

Figure 5

Ukraintsev & Yates

Energy Diagram of p-type Si(001)-(2×1) and Metal Tip

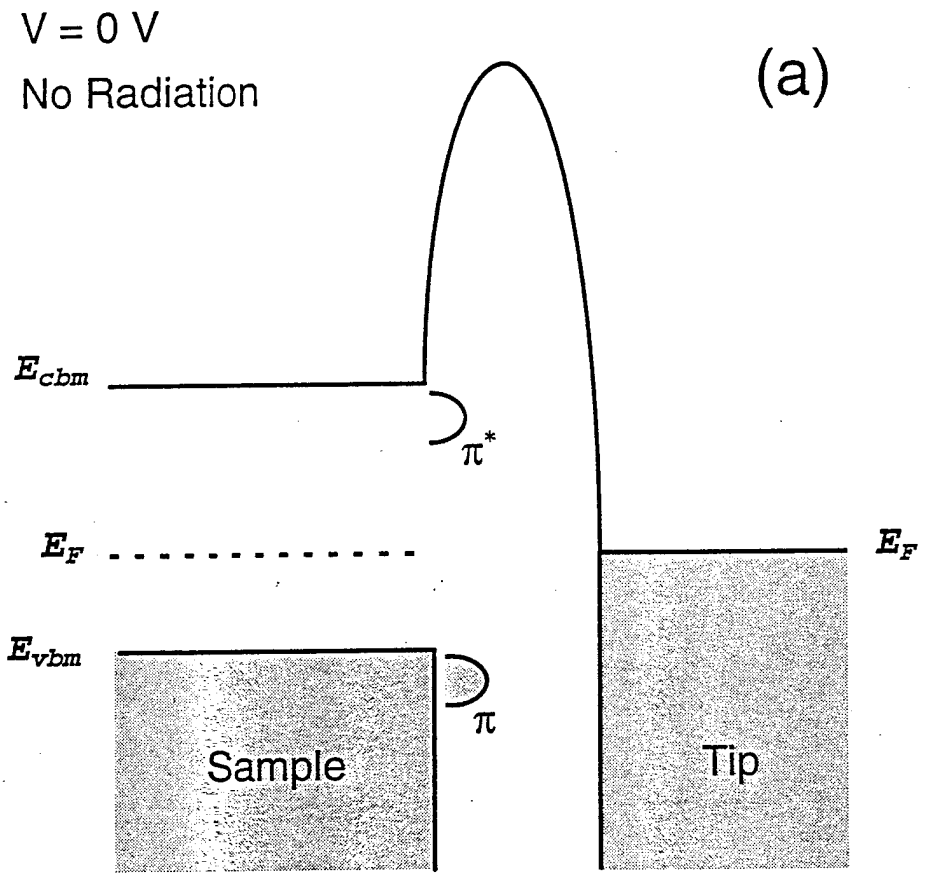

Figure 6(a)
Ukraintsev & Yates

Energy Diagram of p-type Si(001)-(2×1) and Metal Tip

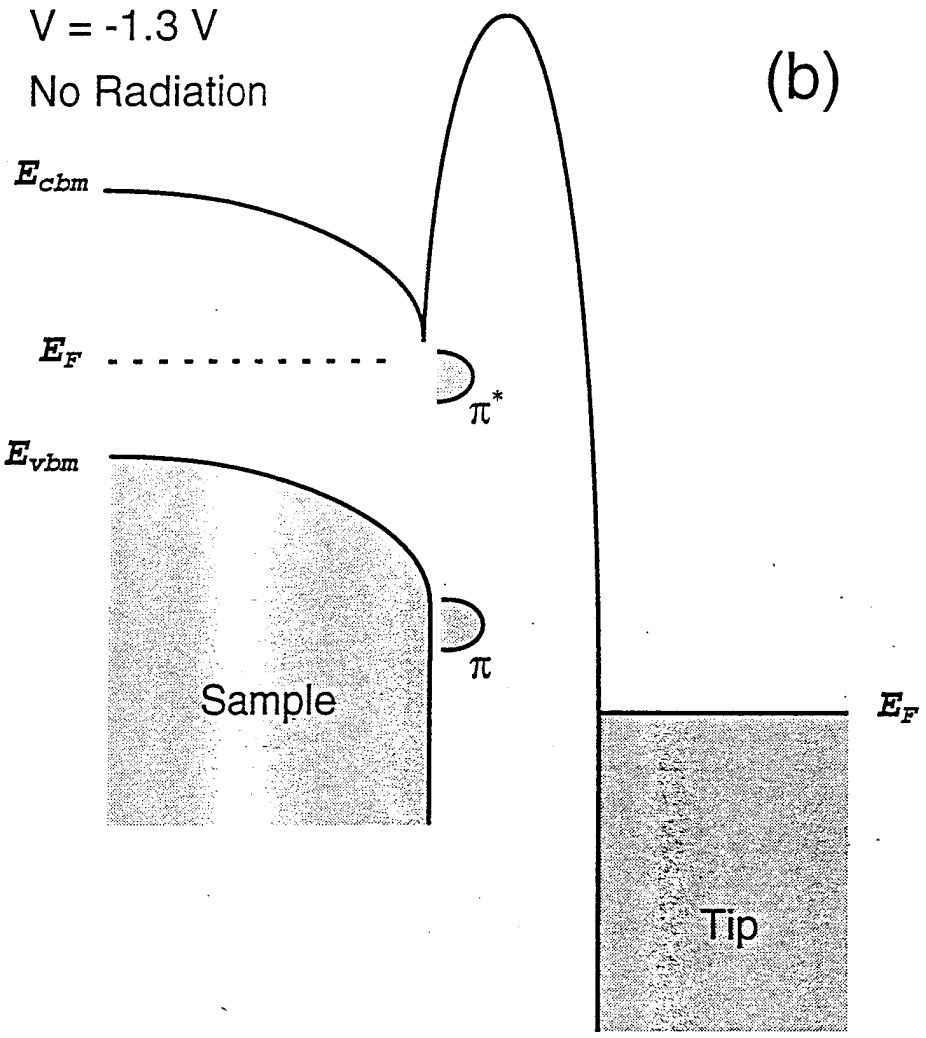

Figure 6(b)
Ukraintsev & Yates

Energy Diagram of p-type Si(001)-(2×1) and Metal Tip

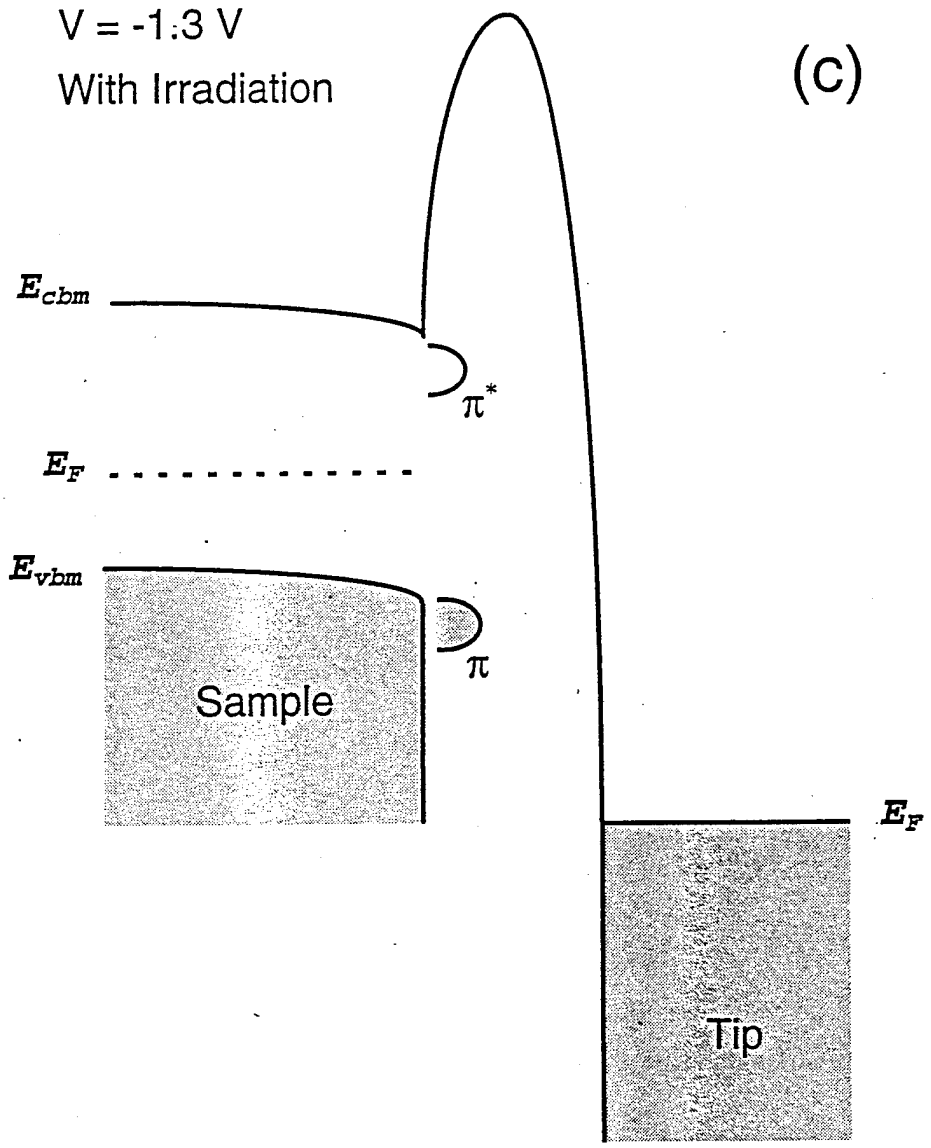

Figure 6(c)
Ukraintsev & Yates

Dr. John C. Pazik (1)*
Physical S&T Division - ONR 331
Office of Naval Research
800 N. Quincy St.
Arlington, VA 22217-5660

Defense Technical Information Ctr (2)
Building 5, Cameron Station
Alexandria, VA 22314

Dr. James S. Murday (1)
Chemistry Division, NRL 6100
Naval Research Laboratory
Washington, DC 20375-5660

Dr. John Fischer (1)
Chemistry Division, Code 385
NAWCWD - China Lake
China Lake, CA 93555-6001

Dr. Peter Seligman (1)
NCCOSC - NRAD
San Diego, CA 92152-5000

Dr. Bernard E. Douda (1)
Crane Division
NAWC
Crane, Indiana 47522-5000

* Number of copies required